WPEDU-PR(17) 18622

B. M. Berger et al.

Sputtering measurements using a quartz crystal microbalance as a catcher

Preprint of Paper to be submitted for publication in
Nuclear Instruments and Methods in Physics Research
Section B

This work has been carried out within the framework of the EUROfusion Consortium and has received funding from the Euratom research and training programme 2014-2018 under grant agreement No 633053. The views and opinions expressed herein do not necessarily reflect those of the European Commission.

This document is intended for publication in the open literature. It is made available on the clear understanding that it may not be further circulated and extracts or references may not be published prior to publication of the original when applicable, or without the consent of the Publications Officer, EUROfusion Programme Management Unit, Culham Science Centre, Abingdon, Oxon, OX14 3DB, UK or e-mail Publications.Officer@euro-fusion.org

Enquiries about Copyright and reproduction should be addressed to the Publications Officer, EUROfusion Programme Management Unit, Culham Science Centre, Abingdon, Oxon, OX14 3DB, UK or e-mail Publications.Officer@euro-fusion.org

The contents of this preprint and all other EUROfusion Preprints, Reports and Conference Papers are available to view online free at http://www.euro-fusionscipub.org. This site has full search facilities and e-mail alert options. In the JET specific papers the diagrams contained within the PDFs on this site are hyperlinked

SPUTTERING MEASUREMENTS
USING A QUARTZ CRYSTAL MICROBALANCE AS A CATCHER

Bernhard M. Berger*, Paul S. Szabo, Reinhard Stadlmayr and Friedrich Aumayr

Institute of Applied Physics, TU Wien, Fusion@ÖAW
Wiedner Hauptstraße 8-10/E134, 1040 Vienna, Austria

Abstract

A quartz crystal microbalance (QCM) catcher setup for sputter yield measurements is described. In this setup a QCM is placed next to the sputter target and acts as a catcher for sputtered material. The sputter yield evaluation relies on assumptions about the angular distribution of sputtered particles and reflected primary projectiles taken from simulations as well as on the knowledge of the sticking coefficient. To test this new setup a second QCM with a Au layer was used as a sputter target. The measured ratio between target and catcher signal is well reproduced in the simulations demonstrating the feasibility of reconstructing the sputtering yield from the catcher signal.

Keywords: Sputtering, Erosion, Quartz-crystal-microbalance, Catcher, Ion-surface interaction

*berger@iap.tuwien.ac.at

1. Introduction

Sputtering due to ion impact is still one of the most important topics of ion-surface interaction [1] with a wide variety of practical applications, like thin-layer deposition, surface etching or surface analytic techniques. It also plays a major role in erosion of wall material in nuclear fusion devices [2] or in space weathering effects observed on lunar or planetary surfaces by solar wind ion impact [3, 4]. A quartz crystal microbalance (QCM) is a common tool to measure mass changes due to ion bombardment. The availability of highly sensitive QCMs offers the unique opportunity to study ion-surface interaction processes in situ and in real time.

At TU Wien sputtering experiments have been performed during the past years by ion bombardment of a thin layer of target material directly deposited on a QCM [5-8]. However, thin layer targets impose a severe restriction on possible experiments, as some target materials cannot easily be deployed in such a form. In particular, composite targets might change their stoichiometry when deposited as a thin layer by evaporation or sputter deposition. Additionally, since the quartz's resonance frequency is strongly temperature dependent, investigations of a possible temperature variation of the sputtering yield become challenging, but would be of great interest, e.g., for wall materials of nuclear fusion devices.

In order to overcome the limitations of such thin layer targets and to open the possibility of using any solid material or even liquids as a sputter target, a new setup was designed, in which the QCM acts as a catcher for sputtered material.

The new setup is introduced in section 2. Since only a fraction of the sputtered material is collected by and sticks to the catcher-QCM, the evaluation of the sputtering yield has to rely on assumptions about the angular distribution of sputtered particles, the fraction and angular distribution of reflected primary projectiles as well as on the knowledge of the sticking coefficient. Our data evaluation is therefore based on input from sputter simulations using the code SDTrimSP [9] as also described in section 2.

In order to confirm the validity of our approach we have used a second QCM with a thin Au layer as a sputter target. We are therefore able to compare the sputtering yields measured with the target-QCM to the one derived from the signal of the catcher-QCM using the input

from the SDTrimSP simulations. Section 3 presents the results of these proof of principle measurements and demonstrates the feasibility of our catcher-QCM method.

2. Experimental Method and Data Evaluation

The schematics of the catcher-QCM setup is shown in figure 1. A sputter target is hit under the angle α with respect to the surface normal by a mass selected ion beam (red arrow from the right). The two shaded areas indicate the angular distribution of the sputtered target particles (blue) and reflected projectiles (red), respectively. At a distance d a QCM is positioned parallel to the ion beam direction, which acts as a catcher for the sputtered material ("catcher-QCM"). The distance between the center of the catcher-QCM (selected to be the x-coordinate origin) and the central strike point of the ion beam on the target is defined as Δx .

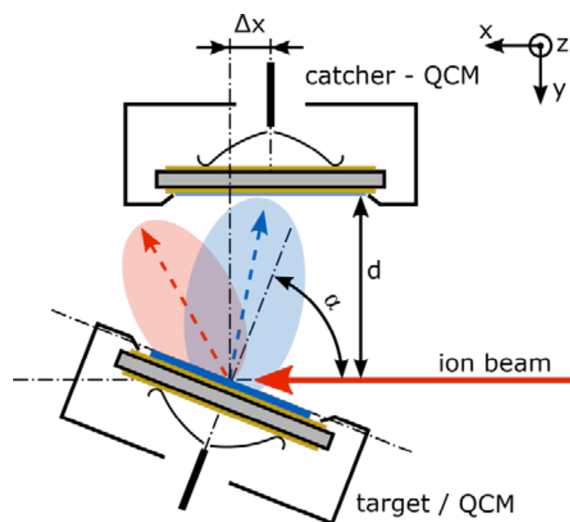

Figure 1 (*1 column width, color online only*)**:** Schematics of the experimental setup. A sputter target (which in our case is a 450 nm Au film on top of one of the gold electrodes of a second QCM, the so called target-QCM) is hit under the angle α by the ion beam (red arrow). The shaded areas indicate the angular distribution of the sputtered target particles (blue) and reflected projectiles (red), respectively. A QCM placed at a distance d from the target parallel to the ion beam direction (with displacement Δx) acts as a catcher for the sputtered material (catcher-QCM).

For the catcher-QCM a plano-convex, stress compensated cut quartz crystal from KVG Quartz Crystal Technology GmbH, Germany is used. This quartz crystal is operated in a driven thickness shear mode at a resonance frequency of about 6 MHz using a highly sophisticated QCM electronics developed at the TU Wien. A detailed description of the used QCM electronics and the QCM technique can be found elsewhere [5, 6].

To test the catcher-QCM configuration a second QCM (target-QCM) with a 450 nm thick Au layer is used instead of a regular target. The Au layer was deposited onto one of the gold electrodes of the quartz crystal (KVG) using a vapor deposition technique. The target-QCM is irradiated by a mass selected Ar^{+} ion beam of 2 keV kinetic energy, produced in a 14.5 GHz all permanent magnet ECR ion source [10]. This configuration with two QCMs allows us to obtain the mass change at the target and at the catcher simultaneously and thus to compare the amount of material sputtered from the target to the amount of material collected by the catcher.

As an example, figure 2 shows the measured resonance frequencies of both QCMs during ion beam irradiation. The measurement starts with a period where the ion beam is interrupted by a shutter to check the frequency drift of the quartz crystals. This is followed by an irradiation period where the ion beam hits the target layer of the target-QCM. During this period, the target-QCM shows an increase of its resonance frequency due to the mass loss from ion-sputtering, while the catcher-QCM shows a decrease of its resonance frequency due to the mass increase from collected sputtered material.

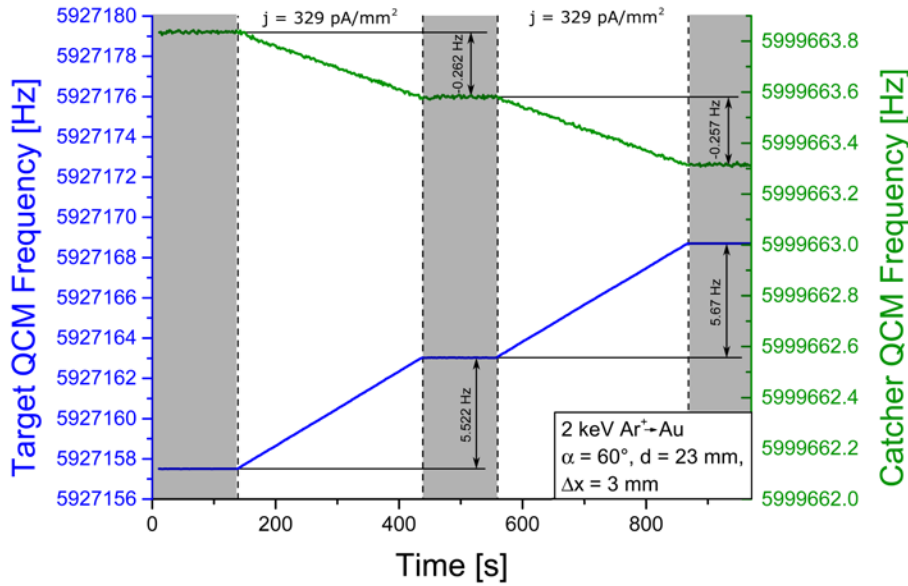

Figure 2 (*2 column width, color online only*)**:** Typical frequency response of the target-QCM and the catcher-QCM to irradiation of a Au layer by 2 keV Ar^+ ions. The geometric parameters of this measurement are $\alpha = 60°$, $d = 23$ mm, $\Delta x = 3$ mm. The measurement starts with a beam-off period (shaded areas) to check the frequency drift of the QCMs (typ. below 2 mHz/min). During the beam-on periods, the target-QCM is irradiated with the ion beam and shows an increase of the resonance frequency due to sputtering (mass decrease), while the catcher-QCM shows a decrease of the resonance frequency due to collected particles (mass increase).

To achieve a uniform irradiation and thereby a uniform thickness change of the target the ion beam is scanned over the quartz crystal´s active area using a pair of deflection plates (for details see ref. [5, 6]). In order to determine the total number of incoming ions the scanned ion beam is controlled with a set of multiple apertures (∅ 2, 3, 4, 7 mm) that can be moved into the beam´s path, directly in front of the target layer. The ion current is then measured using a Faraday cup at the target´s position.

Since the thickness change of the deposited layer is uniform and the layer is very thin compared to the quartz crystal, the Sauerbrey equation can be used. It describes the relation between the relative change of the resonance frequency $\Delta f / f$, thickness $\Delta d / d$ and mass $\Delta m / m$ of the quartz crystal [11]

$$\frac{\Delta f}{f} = -\frac{\Delta d}{d} = -\frac{\Delta m}{m} \tag{1.1}$$

For the target-QCM with the Au layer the sputtering yield Y_{tar} can be evaluated straightforward using the following relation [5]

$$Y_{tar}[\text{atoms/ion}] = \frac{y}{m_t} = \frac{e_0 q}{m_t} \cdot \frac{\rho_Q l_Q}{f_Q m_n} \cdot \frac{\Delta f}{\Delta t} \cdot \frac{1}{j} \tag{1.2}$$

With y being the sputtering yield in amu/ion, m_t the target particle mass in amu, e_0 the electron charge, q the projectile charge state, ρ_Q the mass density of the quartz, l_Q the thickness of the quartz, f_Q the resonance frequency of the quartz, m_n the atomic mass unit, $\Delta f / \Delta t$ the frequency change per time (slope in figure 2) and the ion current density j (for more details see [5]).

Evaluation of the sputtering yield from the catcher-QCM signal is less straightforward. The frequency change of the catcher-QCM is more than a factor of 10 smaller than the frequency change of the target-QCM, indicating incomplete collection of the sputtered material. Two main effects contribute to the catcher-QCM signal. Firstly, only a certain fraction of the atoms sputtered from the target will hit the catcher-QCM and stick to its surface ($Y_{c,sp}$). Secondly some of the projectile ions will be reflected from the target surface and lead to erosion of the catcher surface ($Y_{c,r}$). Both processes are schematically indicated in figure 1. The erosion of the catcher surface due to sputtered particles will be neglected due to their comparably low kinetic energy. The measured mass change (yield Y_c) at the catcher-QCM is thus the difference of the mass increase due to collected sputtered particles and the mass decrease due to erosion caused by reflected projectiles:

$$Y_c = Y_{c,sp} - Y_{c,r} \tag{1.3}$$

The yield of collected atoms $Y_{c,sp}$ is proportional to the sputtering yield of the target Y_{tar}, the sticking coefficient C_{st} (probability that sputtered material reaching the catcher surface sticks there) and a parameter g_{sp} outlined further below:

$$Y_{c,sp} = C_{st} \cdot g_{sp} \cdot Y_{tar} \tag{1.4}$$

The parameter g_{sp} comprises the quartz crystal´s local sensitivity to a mass change $s(x_c, y_c)$, the spatial distribution of the sputtered material $f_{sp}(\Omega)$ (with Ω being the solid angle), the

projectile ion current density profile $j(x_t, y_t)$ on the target and the relative position of the catcher and the target characterized by the parameters α , Δx, and d (see figure 1). In order to derive the parameter g_{sp}, we first consider a point shaped ion beam hitting the target and creating a spatial distribution $f_{sp}(\Omega)$ of sputtered atoms with

$$\int_{2\pi} f_{sp}(\Omega) = 1 \tag{1.5}$$

The number of atoms hitting the catcher is then given by the integration of $Y_{tar} \cdot f_{sp}$ over all angles that represent directions intersecting with the catcher quartz surface. To determine the contribution of the integrand to the measured signal f_{sp} has to be weighted with the non-uniform quartz´s sensitivity $s(x_c(\Omega), y_c(\Omega))$ to a get the actual frequency change (for more details about the quartz´s sensitivity see [11-13]). Here x_c and y_c are the local coordinates in the plane of the catcher surface dependent on the polar angle θ and the azimuthal angle ϕ. The position and orientation of the surface result from the catcher´s position and therefore, all the necessary information is included in x_c and y_c. The limited size of the quartz´s active area is described by a Gaussian-like sensitivity $s(x_c(\Omega), y_c(\Omega))$ which has its maximum in the center and is close to zero at the edges of the catcher quartz. Therefore, the integration can be performed over all angles.

In a second step a finite-size projectile ion beam is now considered, where the sputtered atoms do not originate from a point, but from an area around the impact point characterized by the current density profile $j(x_t, y_t)$ with

$$\int_A j(x_t, y_t) dA = I \tag{1.6}$$

Here x_t and y_t are the coordinates at the target surface and I represents the total ion current hitting the target. The spatial distribution of sputtered particles for an expanded ion beam can then be written as

$$\frac{1}{I} \int_A j(x_t, y_t) \cdot f_{sp}(\Omega, x_t, y_t) \, dA \tag{1.7}$$

with $f_{sp}(\Omega, x_t, y_t)$ now being the spatial distribution of sputtered atoms created by a point shaped ion beam originating at the point (x_t, y_t). As a result, the parameter g_{sp} can then be written as:

$$g_{sp} = \frac{1}{I} \int_A \int_{2\pi} j(x_t, y_t) \cdot f_{sp}(\Omega, x_t, y_t) \cdot s(x_c(\Omega), y_c(\Omega)) \, d\Omega dA \tag{1.8}$$

Similarly, the erosion of the catcher surface due to reflected projectiles (yield $Y_{c,r}$) can be described with the parameter g_r and the reflection probability $P_r(\alpha)$ of the projectile ions from the target:

$$Y_{c,r} = g_r \cdot P_r \tag{1.9}$$

Equivalent to f_{sp}, f_r is used to describe the distribution of the reflected ions. However, in contrast to considerations presented before, the absolute number of atoms sputtered from the catcher surface by the reflected projectiles is now of importance, which depends both on the energy and angular distribution $f_r(\Omega, E)$ of the reflected projectiles. This requires the knowledge of the sputtering yield $Y(\alpha_r, E)$ with α_r being the reflected projectiles angle of incidence on the catcher surface and E their impact energy. Taking all aspects into account, an adaption of equation (1.8) leads to the parameter g_r for the reflected projectiles:

$$g_r = \frac{1}{I}\int_A \int_0^\infty \int_{2\pi} j(x_t, y_t) \cdot f_r(\Omega, E, x_t, y_t) \cdot Y(\alpha_r, E) \cdot s(x_c(\Omega), y_c(\Omega)) \; d\Omega dE dA \tag{1.10}$$

The ratio g between the yield at the catcher (Y_c) and the yield at the target (Y_{tar}) can then be described:

$$Y_c = Y_{c,sp} - Y_{c,r} = C_{sp} \cdot g_{sp} \cdot Y_{tar} - g_r \cdot P_r = \left(C_{sp} \cdot g_{sp} - g_r \cdot \frac{P_r}{Y_{tar}} \right) \cdot Y_{tar} = g \cdot Y_{tar} \tag{1.11}$$

$$\Rightarrow \; g = C_{sp} \cdot g_{sp} - g_r \cdot \frac{P_r}{Y_{tar}} \tag{1.12}$$

Equ. (1.11) offers the possibility of deriving the actual sputtering yield at the target (Y_{tar}) from the measured signal/yield (Y_c) at the catcher if the factor g (equ.(1.12)) can be obtained otherwise e.g. from simulations (or experimental calibration). Since in our test setup we have an independent (direct) measurement of the target sputtering yield Y_{tar} available from the target–QCM, the evaluation procedure outlined above can be put to a stringent test.

For simulating sputtering yields three popular Monte Carlo simulation programs are available (SDTrimSP, TRIDYN and SRIM) [14]. We used the SDTrimSP code (where SD stands for static – dynamic and SP for sequential – parallel) [9, 15], which is an extension of the

codes TRIM and TRIDYN and combines the possibilities of both of them. This code describes the interaction of ions bombarding (amorphous) solids based on a binary-collision approximation and allows a wide variety of different input parameters like the used integration method or different interaction potentials (default interaction potential - KrC [16]). While the strengths of SRIM are the simulation of ion ranges, energy loss and damage profiles, SDTrimSP obtains a good quantitative agreement with experimental data in calculating the sputtering yield Y , the reflection probability of the projectile ions P_r as well as their respective angular distributions f_{sp} and f_r (for a detailed comparison of the simulation programs showing the respective strengths and weaknesses see ref. [14]).

Using this input from SDTrimSP together with the knowledge of the quartz´s sensitivity s , the measured current density j and the sticking coefficient C_{st} the ratio g can then be calculated ("simulated ratio g") according to equ.(1.12) and compared to the experimentally measured catcher to target frequency ratio ("experimental ratio g"). In section 3 we will apply this procedure to reconstruct the target yield Y_{tar} from the experimentally determined catcher signal Y_c and compare the result to the directly measured target sputtering yield Y_{tar} .

3. Proof of principle measurements

To show the feasibility of determining sputtering yields by the catcher-QCM method outlined in section 2, proof of principle measurements with the well-known projectile-target combination Ar^+ on Au were conducted. For 2 keV Ar^+ impact under normal incidence on a polycrystalline Au surface a large compilation of literature data gives a sputtering yield of approximately 5 ± 2 atoms/ion [17] which is consistent with our previous measurements using a target-QCM [6, 18]. For the kinetic energy range where we typically perform our sputtering measurements (< 20 keV) the dominating sputtering effect is due to nuclear sputtering (i.e. sputtering due to momentum transfer between projectile and target atoms [17]) while electronic ([17], chapter 2) and potential sputtering [19] can be neglected. For oblique incidence, the sputtering yield increases by up to a factor of 1.5 for impact angles around 60° [1, 20]. The vast majority of sputtered Au atoms will have energies well below 10

eV with a maximum probability around 1 eV [21]. Since for self-sputtering of Au a threshold close to 10 eV was reported by [22, 23], self-sputtering can be safely neglected. At 1 eV impact energy also a sticking coefficient very close to 1 can be safely assumed for Au atoms on a Au surface [23, 24]. To calculate the factor g, however, only simulation results from the code SDTrimSP have been used for consistency.

In figures 3 (a) – (c) the measured and simulated parameter g are compared for a variety of different catcher positions (characterized by Δx and d) and ion impact angles α. Given the fact that there is no free fitting parameter involved in this comparison, the agreement can be considered to be excellent. Figures 3 (d) – (f) compare the sputtering yield directly measured with the target-QCM (using equ.(1.2)) with the sputtering yield reconstructed from the data of the catcher QCM (using the simulated factor g). Again both sets of data are in good agreement. Figure 3 therefore also allows to select optimum parameters for distance d and displacement Δx for future measurements.
The behavior of the ratio g was first investigated for different angles of incidence α on the target. The angular distribution of sputtered atoms shows a maximum in a cone at 45 to 60 degrees [17], depending on the angle of incidence, which coincides with results of the SDTrimSP simulation. As a result, hardly any particles are able to reach the catcher at small angles of incidence α (see figure 3(a)), which also results in a large uncertainty for the reconstructed sputtering yield (see figure 3(d)). For increasing distances d between the catcher and the target the ratio g decreases steadily (see figure 3(b)). This can be explained by the fact that the catcher-QCM only registers sputtered atoms from a smaller solid angle when it is further away from the target. Also for small distances d a modest deviation between the simulated and measured values can be observed which might be due to surface roughness or inhomogeneities in the ion current profile. For distances larger than 20 mm the error bar of the reconstructed yield again increases because less and less material is collected (figure 3 (e)). This is also the case if the displacement Δx between catcher and target becomes too large (figure 3(f)) because then more and more sputtered atoms miss the catcher and result in a smaller signal. The observed asymmetry in figure 3 (c) can be explained by the chosen angle of incidence α of 60° for this measurement.

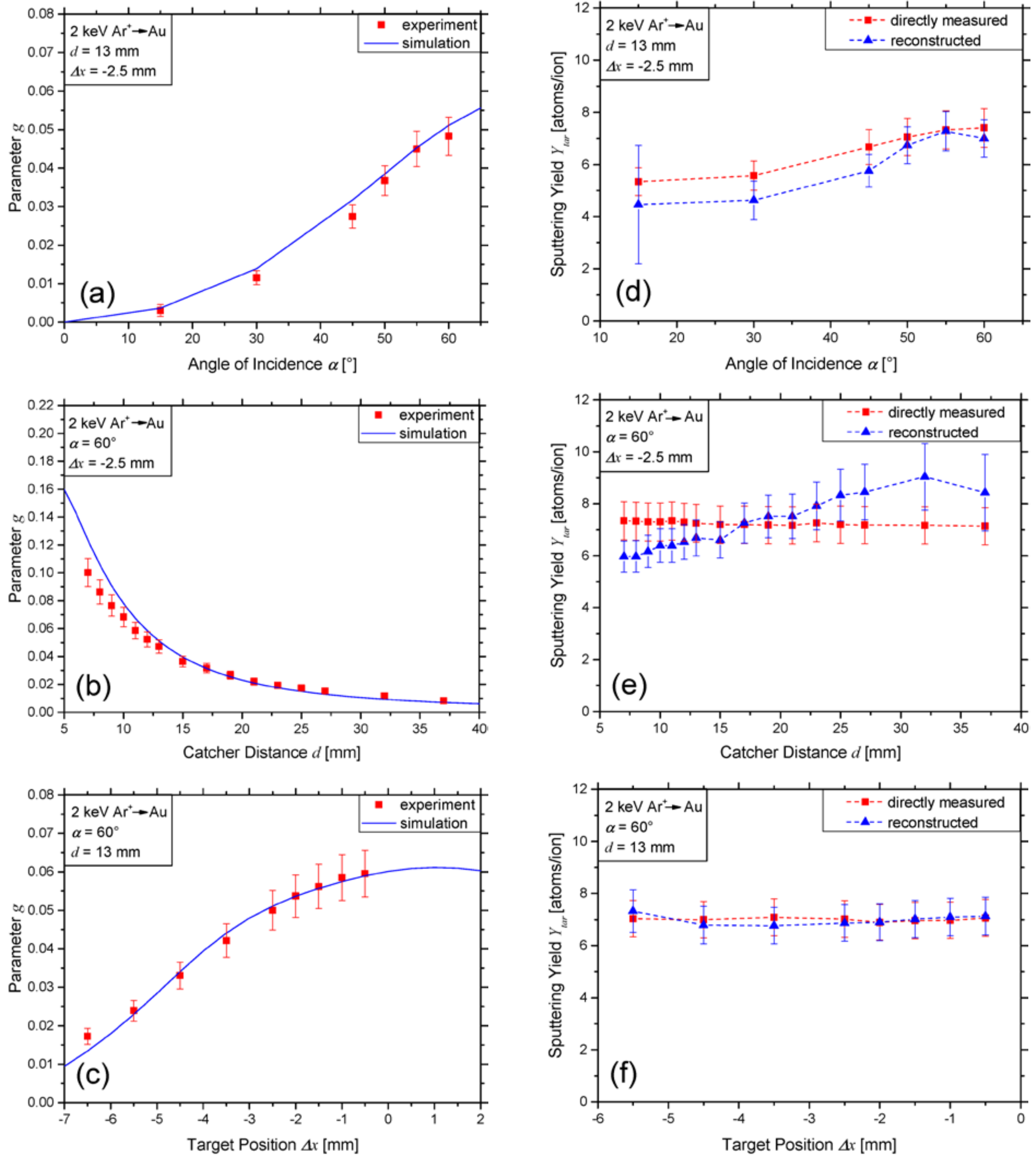

Figure 3 (*2 column width, color online only*): Comparison of the simulated (blue) and measured (red) ratio g **(a - c)** and the measured (Y_{tar}) and reconstructed ($Y_{tar} = Y_c / g$) target sputtering yield **(d - e)** for a variety of different catcher positions (characterized by Δx and d) and ion impact angles α .

4. Summary and outlook

A new experimental setup for the indirect determination of sputter yield has been presented. In this setup a QCM is placed beside the sputter target and acts as a catcher for sputtered material. To link the measured catcher yield to the target sputtering yield, the actual geometry and all relevant processes have been taken into account. Knowledge about the energy and angular distributions of sputtered and reflected particles comes from the simulation code SDTrimSP. To validate this approach proof of principle measurements with the projectile-target combination Ar^+ on Au were performed, in which a second QCM with a Au layer on top acting as a target allows an independent measurement of the sputtering yield. Excellent agreement between both (direct and indirect) methods proves the ability of our new setup to provide absolute sputtering yields.

Future sputter yield measurements in our lab will therefore no longer be limited to thin layer targets pre-deposited on a QCM at a particular temperature favorable for QCM operation [5], but allow experiments with a wide variety of targets (single crystals, compounds and alloys, even liquids) under a range of experimental conditions (effect of temperature or surface morphology) not possible so far. The erosion of wall material in nuclear fusion devices or space weathering effects on lunar or planetary surfaces by ions typical for the solar wind can now be studied on real samples instead of model systems. Compared to other methods used for determining sputtering yields like Rutherford backscattering (RBS) or a weighing technique, the new method is not limited to thin layers targets and can obtain the sputtering yield in situ and in real time. However, with indirectly measuring the sputtering yield, knowledge of the angular distribution of the sputtered material is necessary to reconstruct the absolute sputtering yield.

Acknowledgments

The authors are grateful to Michael Schmid (IAP, TU Wien) for his continued support with the QCM electronics. This work has been carried out within the framework of the EUROfusion Consortium and has received funding from the Euratom research and training programme 2014-2018 under grant agreement No 633053. The views and opinions expressed herein do not necessarily reflect those of

the European Commission. Financial support has also been provided by KKKÖ (commission for the coordination of fusion research in Austria at the Austrian Academy of Sciences - ÖAW).

References

[1] P. Sigmund, Phys. Rev., **184** (1969) 383.

[2] M. Oberkofler, D. Alegre, F. Aumayr, S. Brezinsek, T. Dittmar, K. Dobes, D. Douai, A. Drenik, M. Koppen, U. Kruezi, C. Linsmeier, C.P. Lungu, G. Meisl, M. Mozetic, C. Porosnicu, V. Rohde, S.G. Romanelli, A.U. Team, J.E. Contributors, Fusion Eng. Des., **98-99** (2015) 1371.

[3] H. Hijazi, M.E. Bannister, H.M. Meyer, C.M. Rouleau, A.F. Barghouty, D.L. Rickman, F.W. Meyer, Journal of Geophysical Research: Space Physics, **119** (2014) 8006.

[4] E. Kallio, P. Wurz, R. Killen, S. McKenna-Lawlor, A. Milillo, A. Mura, S. Massetti, S. Orsini, H. Lammer, P. Janhunen, W.H. Ip, Planet. Space Sci., **56** (2008) 1506.

[5] G. Hayderer, M. Schmid, P. Varga, H.P. Winter, F. Aumayr, Rev. Sci. Instrum., **70** (1999) 3696.

[6] A. Golczewski, K. Dobes, G. Wachter, M. Schmid, F. Aumayr, Nucl Instrum Meth B, **267** (2009) 695.

[7] K. Dobes, V. Smejkal, T. Schafer, F. Aumayr, International Journal of Mass Spectrometry, **365** (2014) 64.

[8] B.M. Berger, R. Stadlmayr, G. Meisl, M. Čekada, C. Eisenmenger-Sittner, T. Schwarz-Selinger, F. Aumayr, Nucl. Instr. Meth. Phys. Res. B, **382** (2016) 82.

[9] A. Mutzke, R. Schneider, W. Eckstein, R. Dohmen, SDTrimSP Version 5.00, IPP-Report, 2011.

[10] E. Galutschek, R. Trassl, E. Salzborn, F. Aumayr, H.P. Winter, Journal of Physics: Conference Series, **58** (2007) 395.

[11] G. Sauerbrey, Z. Phys., **155** (1959) 206.

[12] D.S. Stevens, H.F. Tiersten, J. Acous. Soc. Am., **79** (1986) 1811.

[13] M. Schmid, E. Benes, W. Burger, V. Kravchenko, IEEE Trans Ultrason Ferroelectr Freq Control, **38** (1991) 199.

[14] H. Hofsäss, K. Zhang, A. Mutzke, Applied Surface Science, **310** (2014) 134.

[15] W. Möller, W. Eckstein, J.P. Biersack, Comput. Phys. Commun., **51** (1988) 355.

[16] W.D. Wilson, L.G. Haggmark, J.P. Biersack, Physical Review B, **15** (1977) 2458.

[17] R. Behrisch, W. Eckstein, Sputtering by Particle Bombardment, Springer Berlin Heidelberg2007.

[18] G. Hayderer, S. Cernusca, V. Hoffmann, D. Niemann, N. Stolterfoht, M. Schmid, P. Varga, H.P. Winter, F. Aumayr, Nucl Instrum Meth B, **182** (2001) 143.

[19] F. Aumayr, H. Winter, Philosophical transactions. Series A, Mathematical, physical, and engineering sciences, **362** (2004) 77.

[20] A. Oliva-Florio, R.A. Baragiola, M.M. Jakas, E.V. Alonso, J. Ferron, Phys Rev B Condens Matter, **35** (1987) 2198.

[21] G.E. Chapman, B.W. Farmery, M.W. Thompson, I.H. Wilson, Radiat. EIT., **13** (2006) 121.

[22] W.H. Hayward, A.R. Wolter, J. Appl. Phys., **40** (1969) 2911.

[23] K. Ikuse, S. Yoshimura, M. Kiuchi, K. Hine, S. Hamaguchi, Journal of Physics: Conference Series, **106** (2008) 12016.

[24] L. Bachmann, J.J. Shin, J. Appl. Phys., **37** (1966) 242.